Possible Reaction Pathway of $HN_3 + N_5^+$ and Stability of the Products' Isomers

Li Jie Wang,[†] Qian Shu Li,[‡] Peter Warburton,[†] and Paul G. Mezey*[,†]

Department of Chemistry, University of Saskatchewan, 110 Science Place, Saskatoon, SK, S7N 5C9, Canada, and School of Chemical Engineering and Materials Science, Beijing Institute of Technology, Beijing, 100081, China

Received: October 17, 2001

The potential energy surfaces of N_8H^+ involving the synthesis pathway of $N_5^+ + HN_3 \rightarrow N_8H^+$, the isomerization of ortho-$N_8H^+ \rightarrow$ int-N_8H^+, and the decomposition reaction of int-$N_8H^+ \rightarrow N_2H^+ + 3N_2$ were investigated. The structures were optimized by hybrid density functional theory. Relative energies were also calculated using second-order configuration interaction with single and double excitations. The barrier heights of the synthesis pathway in the forward and reverse directions were predicted to be 32.4 and 26.4 kcal/mol, and those of the isomerization and decomposition reactions were 64.9 and 65.3 kcal/mol at the QCISD/6-311++G** level, respectively. A calculation of rate constants for the synthesis and dissociation pathways of N_8H^+ (C_S) was done by the variational transition state theory. The electron densities of species involved in the potential energy surface were calculated and analyzed. The results will provide data for the design of high-energy density materials.

Introduction

With the increasing interest in carbon clusters, other important cluster species have been often overlooked. Many stable structures made of pure nitrogen (N_{2n} and N_{2n+1}) have been predicted theoretically.[1−15] Although N is an isoelectronic analogue to CH and many stable complexes of $(CH)_n$, such as benzene (C_6H_6) and polyalkyne, have been known, most corresponding nitrogen clusters have not been prepared. Since Christe et al.[16] synthesized the AsF_6^- salt of N_5^+ by reacting $N_2F^+AsF_6^-$ with HN_3 in anhydrous hydrogen fluoride at −78 °C in 1998, more and more investigations on all-nitrogen clusters were done. Although a few species were seen for very short periods in gas-phase chemistry, most research of nitrogen clusters is based on theory. Nitrogen clusters are of significant interest as high energy-density materials (HEDMs) for propulsion and explosive applications. The critical properties for effective HEDM molecules are a high dissociation energy barrier and facile syntheses.

The successful experimental synthesis of N_5^+ suggests the combination of the N_5^+ ion with the three-atom azide anion N_3^- to create N_8, a neutral compound. For N_8 isomers, many stable structures have been predicted theoretically.[2−8] Lauderdale et al.[2] studied nitrogen clusters and calculated cubic N_8 clusters with Hartree−Fock self-consistent-field (SCF), coupled cluster (CC), and Møller−Plesset perturbation theory (MP2) methods. From symmetry arguments, they deduced that N_8 should have a significant barrier to decomposition. Their SCF results agree with those of Engelke et al.[4] Glukhovtsev et al.[5] predicted the structures of N_8 isomers, with O_h, D_{2h}, D_{2d}, C_S, C_{2h}, and C_{2v} symmetries. Leininger et al.[6] studied three isomers of N_8 (an octaazacubane structure, a D_{2h} structure analogous to cyclooctatetraene, and a planar bicyclic form analogous to pentalene). The geometries were optimized with SCF, MP2, single and double excitation configuration interaction (CISD), and coupled-cluster method (CCSD) using a DZP basis set. Gagliardi et al. investigated the stability of ten N_8 isomers and the possible dissociation of N_8 to four N_2 molecules.[11,12] To understand the dissociation channels of N_8, they also studied the isomerization reaction from the high-energy azacubane structure to the more stable azapentalene structure. This reaction may occur via a series of intermediate metastable structures with moderately low barriers (10−20 kcal/mol). Five local minima on the potential energy surface (PES) have been found, and the transition states between two neighboring minima have been determined.[8] The potential energy surfaces of N_8 isomers were studied in Chung et al.[15] and our previous works,[17] respectively. Theoretical computational results predicted that combining N_5^+ with N_3^- gives first a quasi-linear N_8 species, then a transfer to N_8 (azidopentazole, C_s) via a series of isomerizations.[15,17−18] It implies that the synthesis of the N_8 (azidopentazole, C_s) is complex and difficult. Therefore, we try to find the synthesis pathways of other compounds containing the N_8 framework.

In all N_8 structures being studied to date, the N_8 (azidopentazole, C_s), formed by a five-membered ring and an open-chain N_3, has the lowest energy predicted for any of the isomers, although its energy is still 197 kcal/mol higher than four N_2 molecules at the B3LYP/6-31+G* level.[5] N_8H^+ is also formed by a five-membered ring and an open-chain N_3 with an ortho-H (or int-H) connected to the ring. Therefore it is worth studying the structures, stability, and syntheses reaction pathway of N_8H^+ (C_s) in order to provide some help for an experiment in synthesizing compounds containing the N_8 (C_s) framework in the future. After we investigated the potential energy surface of the $N_2F^+ + HN_3 \rightarrow N_5^+ + HF$ reaction in theory, with the result of the prediction being in agreement with that of experiment,[19] a possible reaction pathway $N_5^+ + HN_3 \rightarrow N_8H^+$ was designed. In our present work, we studied the PES and rate constants of the N_5^+ (C_{2v}) + HN_3 (C_s) → N_8H^+ (C_s) reaction as well as the isomerization and the stability of isomers of N_8H^+. The stationary points were optimized and the minimum

* Corresponding author. Fax: 1-306-966-4730. Tel: 1-306-966-4661. Email: mezey@sask.usask.ca., wlijie@rhodent.usask.ca.
[†] University of Saskatchewan.
[‡] Beijing Institute of Technology.

10.1021/jp013865n CCC: $22.00
Published on Web 02/09/2002

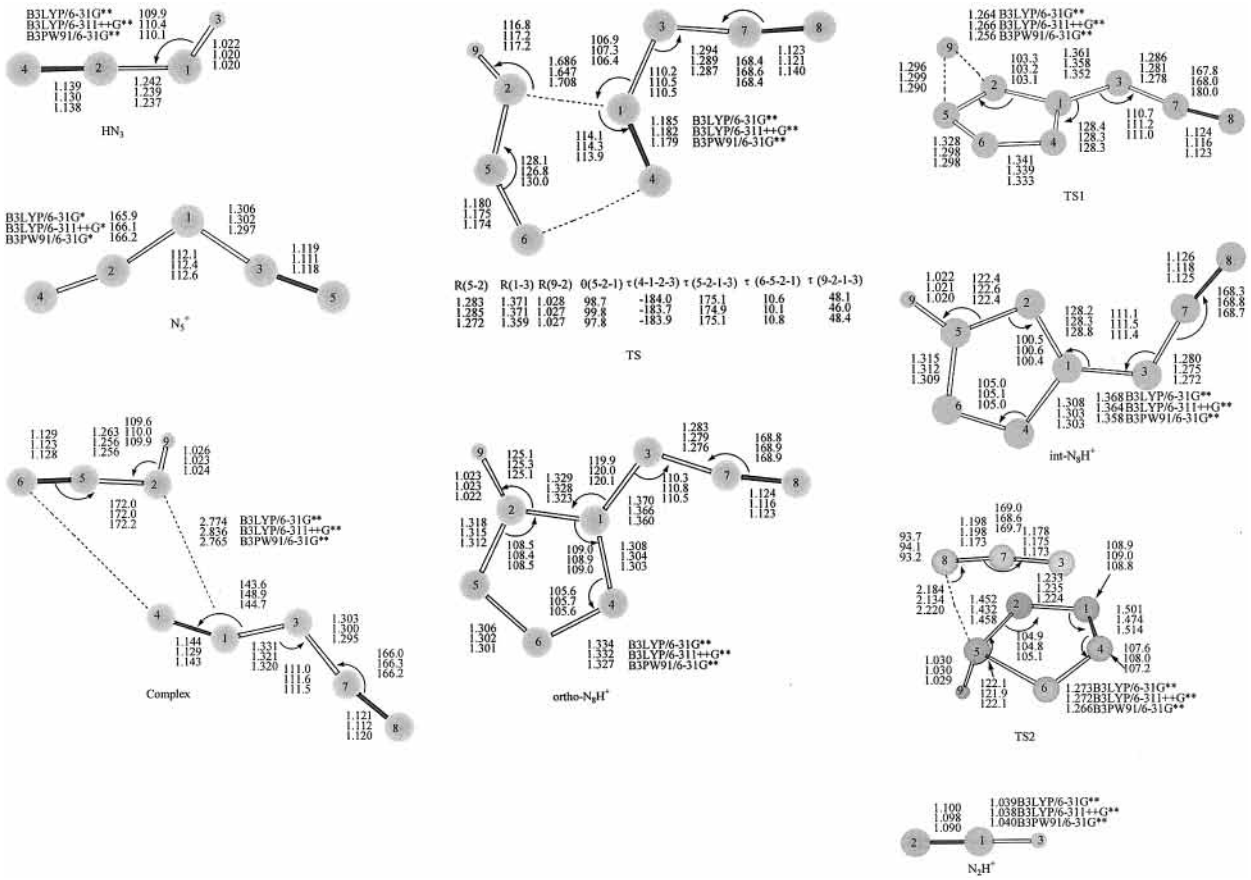

Figure 1. Geometric parameters for various structures involved in the potential energy surface.

energy path (MEP) through mass-scaled coordinates (also called the intrinsic reaction path or intrinsic reaction coordinate, IRC) was calculated. In addition, the reaction rate constants were predicted. These calculations on the ion clusters provide a theoretical foundation for improved design of HEDMs.

Computational Methods

The geometries of N_8H^+ isomers, N_5^+ (C_{2v}), HN_3 (C_s), and the transition states (TS) involved in the reaction of $N_5^+ + HN_3 \rightarrow N_8H^+$ were optimized using hybrid density functional theory (hybrid DFT) methods. The functionals used in the present work comprise the combinations of Becke's three-parameter nonlocal exchange functionals[20] with the nonlocal correlation of Lee, Yang, and Parr[21] and Perdew−Wang 1991 correlation functionals,[22] hereafter denoted as B3LYP and B3PW91. The 6-31G* is a standard split-valence double-ζ polarization basis set, while the 6-311+G* is a split-valence triple-ζ polarization basis set augmented with diffuse functions,[23] both of which were introduced by Pople and co-workers. The relative energies were further calculated using the quadratic configuration interaction calculation, including single and double substitution[24] (QCISD) methods at the QCISD/6-311+G*//B3LYP/6-311+G* level. All calculations were carried out with the Gaussian 98 programs package.[25] To characterize the nature of the stationary points and determine the zero-point energy (ZPE) corrections, harmonic vibrational frequencies were also calculated at the levels of theory mentioned above. Stationary points were identified as either local minima or transition states. To confirm that a given transition state connects reactants and products, minimum energy path calculations[26−30] were performed at the above levels with a coordinate stepsize of 0.1 $(amu)^{1/2}$ bohr.

We also calculated the rate constants with variational transition state theory (VTST)[27] using the tunneling effect corrections of the Wigner[31] (semiclassical transmission coefficient k^W) and MEPSAG[27] (semiclassical adiabatic ground-state method along MEP) methods. The POLYRATE 8.2 program[32] was employed to calculate the theoretical rate constants using VTST theory, and the above two methods (denoted in this paper as TST, TST/W, and TST/MEPSAG, respectively). The forward and reverse synthesis reaction rate constants were obtained by the variational transition state theory at the B3LYP/6-311+G* level of theory for temperature ranges appropriate to those barriers. The electron densities of species involved in the potential energy surface were calculated and analyzed using the Rhocalc2000[33] and MOLCAD II module[34−36] of the SYBY molecular modeling package.[37]

Results and Discussion

The geometric structures of N_8H^+ isomers, complex, transition states, N_5^+, HN_3 and the dissociated products are plotted in Figure 1. Total energies and zero point vibrational energy (ZPVE) are listed in Table 1. The relative energies are presented in Table 2. The main energy relations of potential energy surfaces are shown in Figure 2.

1. The Geometric Structures of N_8H^+ Systems. In the following discussions, we will mainly use the B3LYP/6-311++G** results unless otherwise indicated. The N_5^+ cation has C_{2v} symmetry, while HN_3 has C_s symmetry. The complex is an ion−molecule structure with C_1 symmetry. The structure of the N_8H^+ contains a five-membered ring and an open-chain in addition to ortho-H (or int-H) connecting the ring. The structures TS, TS1, and TS2 are the transition states of the processing $N_5^+ + HN_3 \rightarrow$ orth-N_8H^+, isomerization of int-N_8H^+

TABLE 1: Total Energies (in kcal/mol) and ZPE (in kcal/mol) of Species

	6-31G**		6-311++G**
methods	B3LYP	B3PW91	B3LYP
N_5^+ (D_5h)	−273.28299	−273.17292	−273.35638
ZPVE	12.8	13.0	12.7
HN_3 (C_s)	−164.78584	−164.73152	−164.83599
ZPVE	13.4	13.6	13.4
complex (C_1)	−438.09014	−437.91409	−438.20962
ZPVE	27.3	27.7	27.0
TS (C_1)	−438.04672	−437.87374	−438.16112
ZPVE	28.0	28.4	28.0
ortho-N_8H^+ (C_s)	−438.08669	−437.92049	−438.19705
ZPVE	30.4	31.0	30.2
TS1 (C_1)	−438.00268	−437.83695	−438.11226
ZPVE	26.5	27.1	26.3
int-N_8H^+ (C_s)	−438.10566	−437.94333	−438.21959
ZPVE	31.1	31.6	30.9
TS2 (C_1)	−437.99239	−437.81819	−438.09966
ZPVE	27.3	27.9	27.0
N_2($D_\infty h$)	−109.52413	−109.47710	−109.55969
ZPVE	3.5	3.5	3.5
N_2H^+ ($C_\infty v$)	−109.72176	−109.67642	−109.75350
ZPVE	10.3	10.3	10.3

TABLE 2: Relative Energies (in kcal/mol) Corrected by ZPEs of Species

	6-31G**		6-311++G**	
methods	B3LYP	B3PW91	B3LYP	QCISD[a]
$N_5^+ + HN_3$	12.3	4.9	9.9	7.3
complex	0.0	0.0	0.0	0.0
TS	27.8	26.0	31.4	32.4
ortho-N_8H^+	5.3	7.7	10.7	6.0
TS1	54.0	47.7	60.3	61.2
int-N_8H^+	−5.9	−14.4	−2.4	−3.7
TS2	61.3	60.4	69.0	65.3
$3N_2+N_2H^+$	−134.5	−128.4	−146.8	−182.4

[a] Single point energy corrected by B3LYP ZPEs was calculated at the QCISD/6-311++G**// B3LYP/6-311++G** level.

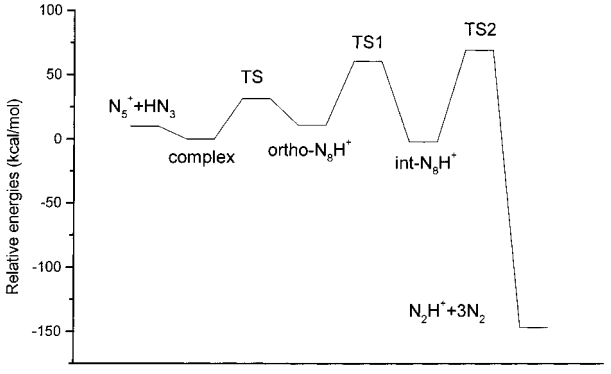

Figure 2. Potential energy surface of N_8H^+ system at the B3LYP/6-311++G** level.

→ ortho-N_8H^+, and dissociated reaction of int-N_8H^+ → $3N_2$ + N_2H^+ all with C_1 symmetry. The dissociated product N_2H^+ is a positive ion with C_{8v} symmetry.

2. The PES of N_8H^+. *A. $N_5^+ + HN_3$ → Complex → TS → ortho-N_8H^+.* In the forward direction, the starting point in the mechanism is the formation of an ion−molecule complex. When the molecule HN_3 and positive ion N_5^+ collide with each other, the N1 and N4 atoms in N_5^+ mainly attack the N2 and N6 atoms in HN_3, respectively. The complex can be formed with no activation energy barrier. As shown in Figure 2 and Table 2, the complex is more stable than the reactants ($N_5^+ + HN_3$). With the bond lengths of N1−N2 and N4−N6 becoming shorter, the intermediate (complex) changes into the structure ortho-N_8H^+ via TS.

In this transition structure (TS), the bond distance of N1−N2 is shortened, at the same time the N6−N4 distance is also shortened. The transition structure is verified as being a saddle point 1 on the PES[38] for it has one imaginary vibrational frequency. The structures along the PES of the forward direction change with the bond lengths of N1−N2 and N6−N4 shortening. Finally, the bonds N1−N2 and N4−N6 are formed by coloumb force, that is, ortho-N_8H^+ is formed. Based on the energy difference between the complex and the TS at different levels, the reaction barrier heights are in the range 26.0−32.4 kcal/mol.

The complex is a local minimum (see Figure 2) on the PES having only real harmonic vibrational frequencies at the above-mentioned levels of theory. The local negative charges are found on the N2 atom, while the positive charges in N_5^+ all mainly concentrate on the N1 atom. The long distance between the N1 and N2 atoms suggests that the charge attraction force between N1 and N2 is weakened.

In the reverse reaction, the N1−N2 and N4−N6 bond lengths in the complex change greatly in the course of reaction, while those of the others change only slightly. Therefore, the N1−N2 and N4−N6 bonds would break and N_8H^+ (C_s) would dissociate into two species: $N_5^+ + HN_3$. In the complex, the sum of charges on atoms N5, N6, N2, and H9 is +0.2 e based on a natural bond orbital (NBO) analysis, corresponding to that of product HN_3, and that on atoms N1, N3, N4, N7, and N8 is +0.8 e, corresponding to that of product N_5^+. In other words, most of the positive charge is on the N1−N3−N4−N7−N8 species. To confirm that the products are N_5^+ and HN_3, the charge distributions were calculated again when the bond length of N1−N2 was lengthened from 2.8 to 6.0 Å and the other parameters were not changed. The calculated results imply that the positive charge distributes mainly on the part of N_5^+ and the charge on HN_3 is small. The result agrees with that from BNO analysis, which suggests that the bonds N6−N5, N7−N8, and N1−N4 are triple bonds, while N4−N6 and N1−N2 are broken bonds. Therefore, we believe that ortho-N_8H^+ indeed dissociates into N_5^+ and HN_3, and does not dissociate into a pair of neutral radicals or two ions. The barrier height of dissociation is 20.7 kcal/mol, and it was further calculated at the QCISD/6-311++G**//B3LYP/6-311++G** level to be 26.4 kcal/mol. The decomposition of the N_8H^+ cluster is an exothermic reaction. All of our calculations predict the energy released of the whole reaction as being 5.3−10.7 kcal/mol with ZPVE corrections.

To verify that the transition state really connects the complex and the ortho-N_8H^+, IRC calculations were also performed starting from each corresponding transition state at the levels of B3LYP/6-31G** and B3LYP/6-311++G**, respectively. The geometries of the two species obtained from these IRC calculations are very close to those from the geometry optimization calculations.

Therefore, the synthesis reaction of the ortho-N_8H^+ (C_s) cluster by N_5^+ and HN_3 is an endothermic reaction. Our calculations predict that the endothermic heat of the whole reaction is 6.0 kcal/mol at the QCISD/6-311++G**//B3LYP/6-311++G** level.

B. Isomerization of ortho-N_8H^+ → TS1 → int-N_8H^+. In the second part of the study, the PES of the N_8H^+ isomerization was investigated. The atom H9 transfers from atom N2 to atom N5. The barrier of isomerization from ortho-N_8H^+ to int-N_8H^+ is 64.9 kcal/mol at the level of QCISD/6-311++G**// B3LYP/

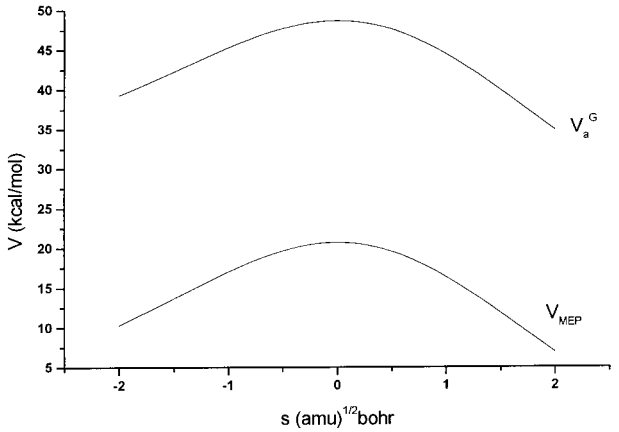

Figure 3. Potential energy curve (V_{MEP}) and the vibrationaly adiabatic ground-state potential energy curve (V_aG) as functions of the intrinsic reaction coordinate s (amu$^{1/2}$ bohr) at the QCISD/6-311++G**// B3LYP/6-311++G** level.

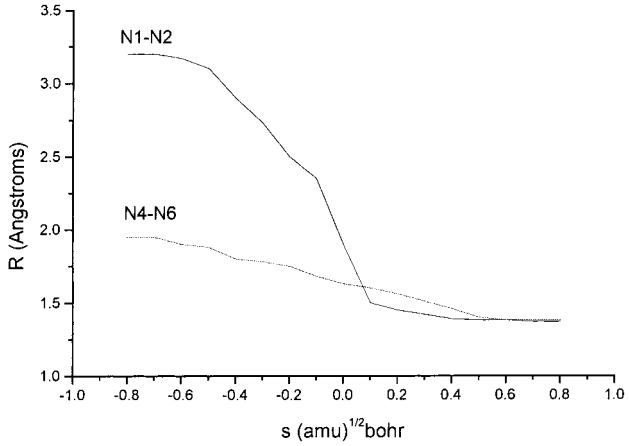

Figure 4. Changes of the main bond lengths as functions of instrinsic reaction coordinate s at the B3LYP/6-311++G* level.

6-311++G**. It is higher than that of synthesis, that is, the synthesis reaction will occur more easily than that of the isomerization.

C. The Dissociation Reaction of int-N_8H^+. The ion int-N_8H^+ dissociates into four species: $3N_2 + N_2H^+$ via TS2, and the dissociation barrier is 71.4 kcal/mol. The results of the Mulliken population analysis show that the charge on H9+N5+N8 is +0.85 e, those on N7+N3, N6+N4, and N1+N2 are +0.07, +0.1 and −0.02 e, respectively. These results imply that the principal positive change is on the species H9+N5+N8 (corresponding to that of HN_2^+), and the other three species are almost the same as the neutral molecules (corresponding to $3N_2$). The higher barrier of int-N_8H^+ dissociation implies that int-N_8H^+ is more stable.

3. The Synthesis Reaction Rate Constants. The MEP was calculated at the B3LYP/ 6-311++G** level from the TS to both the complex and the product channels. It was refined with the QCISD method to obtain a more reliable potential energy curve. The validity of this correction procedure, called VTST-ISPE, has been studied elsewhere.[39] Classsical energies along the MEP, V_{MEP}, and the ground-state vibrationally adiabatic potential curve, V_aG, which is the sum of V_{MEP} and the ZPE, are plotted as functions of *s* in Figure 3. It can be seen that the V_{MEP} and V_aG curves are similar in shape, and this implies that the vibrational effect for the calculation of the rate constants is small. The maximum values for the two potential energy curves

TABLE 3: Synthesis Forward Reaction Rate Constants (in cm^3 mol^{-1} s^{-1})

T (K)	TST	TST/W	TST/MEPSAG
435.0	9.7E+03	1.1E+04	1.1E+04
600.0	4.4E+06	4.7E+06	4.7E+06
1000.0	3.9E+09	4.0E+09	4.0E+09
1500.0	1.2E+11	1.2E+11	1.2E+11

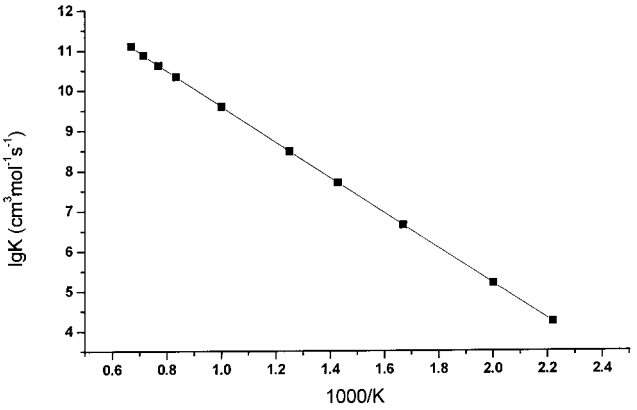

Figure 5. Arrhenius plot of the forward reaction rate constant (cm^3 mol^{-1} s^{-1}) for the $N_5^+ + HN_3 \rightarrow N_8H^+$ reaction in the temperature range 435−1500 K.

TABLE 4: Synthesis Reverse Reaction Rate Constants (in cm^3 mol^{-1} s^{-1})

T (K)	TST	TST/W	TST/MEPSAG
435.0	2.0E−06	2.2E−06	2.2E−06
600.0	4.2E−02	4.4E−02	4.4E−02
1000.0	1.4E+03	1.4E+03	1.4E+03
1500.0	2.5E+05	2.5E+05	2.5E+05

occur at the same position. The maxima of V_aG and V_{MEP} are located at about $s = 0.0$ (amu)$^{1/2}$ bohr.

The bond length changes of the reaction system along the MEP are described in Figure 4. It could be seen that the geometric changes mainly take place in the region from about $s = -0.1$ to 0.6. With the bonds N1−N2 and N4−N6 formed in the forward direction, N_8H^+ is synthesized from N_5^+ and HN_3.

To carry out the variational transition state theory (VTST) calculation, we selected eight points near the transition state region along the MEP between the complex and product channel, respectively. For the purpose of comparison, TST, TST/W, and TST/MEPSAG were performed to obtain both the forward and reverse reaction rate constants in the temperature range from 435 to 1500 K. The rate constants are shown in Tables 3 and 4. It can be seen that the forward reaction does not occur appreciably, while the reverse reaction happens readily at room temperature. The result corresponds to that of energy barriers hindering the forward reaction. The TST rate is near to the TST/W and TST/MEPSAG rates, confirming that the variational effect for the calculation of the rate constants is small.

4. Analysis of Electron Densities of Species in N_8H^+ System. The electron densities of complex, TS, orth-N_8H^+ and fragments HN_3 and N_5 were calculated and their images are shown in Figure 6. We choose one threshold value of density (0.1 au) to analyze the change of electron density along the N_8H^+ PES. From the reaction process of complex → TS → orth-N_8H^+ and the change of electron density shapes of the fragments HN_3 and N_5 at the same threshold value (0.1 au), one concludes that the shapes of electron density of atoms 1, 4, 2, 5, and 6 changed greatly, while the bonds between atoms N1 and N2, N4 and N6 were formed. The five-membered ring

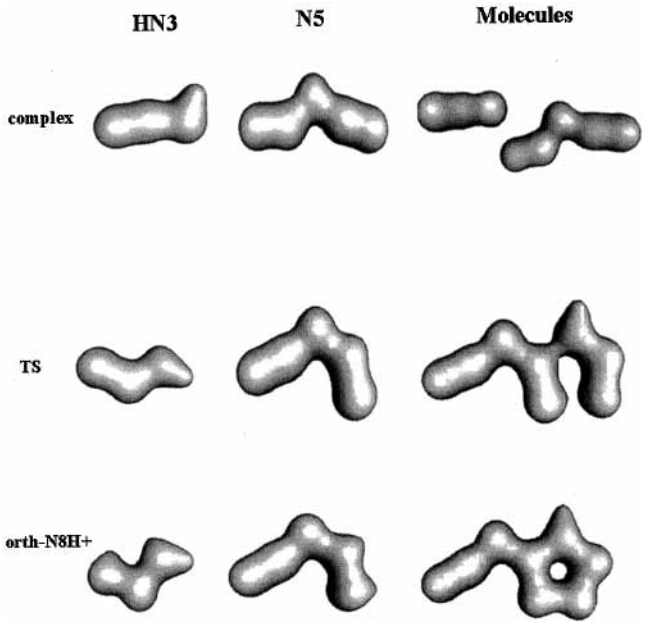

Figure 6. Approximate isodensity surfaces constructed using the Rhocalc program for the value 0.1 am of threshold density for the species on the PES of N_8H^+ system.

in the whole molecule N_8H^+ is formed by two atoms of N_5^+ and three atoms of HN_3. The results of electron density analysis agree with that of the IRC study. Therefore, we conclude that the synthesis pathway of N_8H^+ obtained by the above two methods appears reliable.

Summary

All of our calculations on the PES of the isomerization reaction, the rate constants of synthesis and decomposition, and the stability of N_8H^+ isomers showed that the synthesis of ortho-N_8H^+ (C_s) by N_5^+ and HN_3 is an endothermic reaction and the decomposition of ortho-N_8H^+ (C_s) is an exothermic reaction. The reliability of the synthesizing reaction pathway has been proved by analysis of both the electron density and IRC. The modestly high barrier of decomposition (26.4 kcal/mol) suggests that the effectiveness of ortho-N_8H^+ as a HEDM molecule is marginal. The higher barrier heights of the isomerization and dissociations imply that N_8H^+ is more stable. Therefore, the investigation of the PES provides a theoretical foundation for understanding the decomposition and synthesis mechanism of N_8H^+, as well as suggesting the possibility of N_8H^+ as a HEDM molecule.

Acknowledgment. The authors thank Professor D. G. Truhlar for providing the Polyrate 8.2 program. The financial support of the National Sciences and Engineering Research council (NSERC) Canada, in the form of both operating of strategic research grants to Paul G. Mezey are gratefully acknowledged.

References and Notes

(1) Pyykkö, P.; Runeberg, N. *J. Mol. Struct. (THEOCHEM)* **1991**, *234*, 279.
(2) Lauderdale, W. J.; Stanton, J. F.; Bartlett, R. J. *J. Phys. Chem.* **1992**, *96*, 1173.
(3) Gimarc, B. M.; Zhao, M. *Inorg. Chem.* **1996**, *35*, 3289.
(4) Engelke, R.; Stine, J. R. *J. Phys. Chem.* **1990**, *94*, 5689.
(5) Glukhovtsev, M. N.; Jiao, H.; Schleyer, P. v. R. *Inorg. Chem.* **1996**, *35*, 7124.
(6) Leininger, M. L.; Sherrill, C. D.; Schaefer, H. F. *J. Phys. Chem.* **1995**, *99*, 2324.
(7) Tian, A.; Ding, F.; Zhang, L.; Xie, Y.; Schaefer, H. F. *J. Phys. Chem. A* **1997**, *101*, 1946.
(8) Gagliardi, L.; Evangelisti, S.; Widmark, P.-O.; Roos, B. O. *Theor. Chem. Acc.* **1997**, *9*, 136.
(9) Wang, X.; Hu, H.-Y.; Tian, A.; Wong, N. B.; Chien, S.-H.; Li, W.-K. *Chem. Phys. Lett.* **2000**, *329*, 483.
(10) Gimarc, B. M.; Zhao, M. *Inorg. Chem.* **1996**, *35*, 3289.
(11) Gagliardi, L.; Evangelisti, S.; Roos, B. O.; Widmark, P.-O. *Theochem.* **1998,** *428*, 1.
(12) Gagliardi, L.; Evangelisti, S.; Bernhardsson, A.; Lindh, R.; Roos, B. O. *Int. J. Quantum Chem.* **2000**, *77*, 311.
(13) Li, J.; Liu, C.-W.; LU, J.-X. *Theochem.* **1993**, *99*, 223.
(14) Wang, X.; Tian, A.; Wong, N. B.; Law, C.-K.; Li, W.-K. *Chem. Phys. Lett.* **2001**, *338*, 3670.
(15) Chung, G.; Schmidt, M. W.; Gordon, M. S. *J. Phys. Chem. A* **2000**, *104*, 5647.
(16) Christe, K. O.; Wilson, W. W.; Sheehy, J. A.; Boatz, J. A. *Angew. Chem.* **1999**, *38*, 2004.
(17) Wang, L. J.; Li, S.; Li, Q. S. *Comput. Chem.* **2001**, *22*, 1334.
(18) Li, Q. S.; Wang, L. J. *J. Phys. Chem. A* **2001**, *105*, 1979.
(19) Xu, W. G.; Li, G. L.; Wang, L. J.; Li, S.; Li, Q. S. *Chem. Phys. Lett.* **1999**, *314*, 300.
(20) Becke, A. D. *J. Chem. Phys.* **1993**, *98*, 5648.
(21) Lee, C.; Yang, W.; Parr, R. G. *Phys. Rev. B* **1988**, *37*, 785.
(22) Perdew, J. P.; Wang, Y. *Phys. Rev. B* **1992**, *45*, 13244.
(23) Hehre, W. J.; Radom, L.; Schleyer, P. v. R.; Pople, J. A. *Ab Initio Molecular Orbital Theory*; Wiley & Sons: New York, 1986.
(24) Pople, J. A.; Head-Gordon, M.; Raghavachari, K. *J. Chem. Phys.* **1987**, *87*, 5968.
(25) Frisch, M. J.; Trucks, G. W.; Schlegel, H. B.; Robb, M. A.; Cheeseman, J. R.; Zakrzewski, V. G.; Montgomery, J. A.; Stratmann, R. E.; Burant, J. C.; Dapprich, S.; Millam, J. M.; Daniels, A. D.; Kudin, K. N.; Strain, M. C.; Farkas, O.; Tomasi, J.; Barone, V.; Cossi, M.; Cammi, R.; Mennucci, B.; Pomelli, C.; Adamo, C.; Clifford, S.; Ochterski, J.; Petersson, G. A.; Ayala,. P. Y.; Cui, Q.; Morokuma, K.; Malick, D. K.; Rabuck, A. D.; Raghavachari, K.; Foresman, J. B.; Cioslowski, J.; Ortiz, J. V.; Stefanov, B. B.; Liu, G.; Liashenko, A.; Piskorz, P.; Komaromi, I.; Gomperts, R.; Martin, R. L.; Fox, D. J.; Keith, T.; Al-Laham, M. A.; Peng, C. Y.; Nanayakkara, A.; Gonzalez, C.; Challacombe, M.; Gill, P. M. W.; Johnson, B.; Chen, W.; Wong, M. W.; Andres, J. L.; Gonzalez, C.; Head-Gordon, M.; Replogle, E. S.; Pople, J. A. *Gaussion 98*, rev. A.5; Gaussian, Inc.: Pittsburgh, PA, 1998.
(26) Melissas, V. S.; Truhlar, D. G.; Garrett, B. C. *J. Chem. Phys.* **1992**, *96*, 5758.
(27) Truhlar, D. G.; Garrett, B. C. *Acc. Chem. Res.* **1980**, *13*, 440.
(28) Fukui, K. *Acc. Chem. Res.* **1981**, *14*, 363.
(29) Gonzalez, C.; Schlegel, H. B. *J. Chem. Phys.* **1989**, *90*, 2154.
(30) Gonzalez, C.; Schlegel, H. B. *J. Phys. Chem.* **1990**, *94*, 5523.
(31) Dupuis, M. J.; Lester, W. A., Jr.; Lengsfield, B. H.; Lui, B. *J. Chem. Phys.* **1983**, *79*, 6167.
(32) Chuang, Y.-Y.; Corchado, J. C.; Fast, P. L.; Villa, J.; Hu, W. P.; Liu, Y. P.; Lynch, G. C.; Jackels, C. F.; Nguyen, K.; Gu, M. Z.; Rossi, I.; Coitino, E.; Clayton, S.; Melissas, V. S.; Steckler, R.; Garrett, B. C.; Isaacson, A. D.; Truhlar, D. G. *Polyrate*, University of Minnesota, MN, 1998.
(33) Warburton, P.; Walker, P. D.; Mezey, P. G. *Rhocalc2000* program, Mathematical Chemistry Research, University of Saskatchewan, 2000.
(34) Brickmann, J.; Keil, M.; Exner, T. E.; Marhöfer, R. *J. Mol. Model.* **2000**, *6*, 328−340.
(35) Waldherr-Teschner, M.; Goetze, T.; Heiden, W.; Knoblauch, M.; Vollhardt, H.; Brickmann, J. *MOLCAD - Computer Aides Vizualization and Manipulation of Models in Molecular Science*; Second Eurographics Workshop on Visualization in Scientific Computing, Delft, Netherlands, 1991.
(36) Brickmann, J.; Keil, M.; Exner, T. E.; Marhöfer, R.; Moeckel, G. *The Encyclopedia of Computation Chemistry*; Schleyer, P. v. R., Allinger, N. C., Clark, T., Gasteiger, J., Kollmann, P. A., Schaefer III, H. F., Schreiner, P. R., Eds.; John Wiley & Sons: Chichester, 1998; pp 1679−1693.
(37) SYBYL 6.7, Tripos Inc., 1699 South Hamley Road, St. Louis, MO 63144, 2000.
(38) Mezey, P. G. *Potential Energy Hypersurfaces*; Elsevier: Amsterdam, 1987.
(39) Chuang, Y.-Y.; Corckodo, J. C.; Truhlar, D. G. *J. Phys. Chem. A* **1999**, *103*, 1140.